



CORONAVIRUS Diagnosis Based on Chest X-Ray Images and Pre-trained DenseNet-121



Yousra Kateb ^{a,1,*}, Hocine Meglouli ^a, Abdelmalek Khebli ^a

^a Faculty of Hydrocarbons and Chemistry, University of M'hamed Bougarra Boumerdes, Algeria

¹ shoffans@upnyk.ac.id

* Corresponding Author

ARTICLE INFO

Article history

Received Sept 12, 2021

Revised Oct 20, 2021

Accepted Nov 30, 2021

Keywords

Covid-19 Diagnosis

DenseNet-121

Chest X-Ray

Image Classification

Convolutional Neural Network

ABSTRACT

A serious global problem called COVID-19 has killed a great number of people and rendered many projects useless. The obtained individual's identification at the appropriate time is one of the crucial methods to reduce losses. By detecting and recognizing contaminated individuals in the early stages, artificial intelligence can help many associations in these situations. In this study, we offer a fully automated method to identify COVID-19 from a patient's chest X-ray images without the need for a clinical expert's assistance. A new dataset was released, which consists of 300 chest X-ray images from 100 healthy individuals, 100 individuals who were infected with Covid 19, and 100 images of viral pneumonitis. 100 more for testing, too. In order to attain an F1 score of 0.98, a Recall of 0.98, and also an Accuracy of 0.98 with this dataset, a classification method deep learning-based learning algorithm DenseNet-121, transfer learning, as well as data augmentation techniques were implemented. Therefore, even though there are not enough training photos, these findings are far better than other state-of-the-art.

This is an open access article under the [CC-BY-SA](https://creativecommons.org/licenses/by-sa/4.0/) license.



1. Introduction

As of June 8 in 2021, CORONAVIRUS disease 2019 (COVID-19), an infectious disease, had infected more than 174 million people worldwide and claimed more than 3.74 million lives [1]. The inefficiency and lack of diagnostics is one of the biggest obstacles to stopping the development of this disease. Reverse transcription polymerase chain reaction is the primary technology used in current tests (RT-PCR). In comparison to the COVID-19 rapid spreading rate, it takes four to six hours to receive the results. In addition to being ineffective, RT-PCR test units are extremely scarce. As a result, many infected instances cannot be easily identified and continue to unintentionally infect others. While (RT-PCR) has been regarded as the best quality level for SARS-CoV-2 analysis, the extremely limited stock and strict requirements for research facility climate would extraordinarily defer the precise finding of suspected patients, which has presented remarkable difficulties to stop the spread of the infection, especially at the focal point of the pandemic region. It's interesting that by combining the patient's clinical signs and symptoms with their new close contact, travel background, and research center findings, X-ray chest image diagnosis is a quick and efficient and simpler technique for clinical conclusion of COVID-19. This makes it possible for a quick determination as

ahead of schedule as possible in the clinical practice. It is also helpful in controlling the plague, especially inside the confines of Wuhan, Hubei area, by timely removing affected patients. In other words, a chest X-ray is a crucial part of the symptomatic technique for suspected patients, and several recent papers have highlighted its symptoms.

[2]–[6] Deep learning, the primary advancement of the recently developing artificial intelligence (AI), has been accounted for in clinical imaging for the preprogrammed detection of lung diseases [7]–[9]. It demonstrated dermatologist-level performance on ordering skin lesions in 2017 [10], outperformed human-level execution on the ImageNet image classification task with 1,000,000 pictures for training in 2015 [11], and obtained remarkably good results for cellular breakdown in the lungs separating 2019 [7]. As a result, our goal is to apply a deep learning model to determine whether COVID-19 is present in the X-ray pictures or not. The Densely Connected Convolutional Networks DenseNet121 model will be used in this study because of its benefits, including high accuracy, capacity, parameter efficiency, and the ability to address the overfitting issue.

This paper is structured as follows: The most recent and well-liked relevant works are reviewed in Section 2, our approach is put into practice in Section 3, and the results and discussion are covered in Section 4. Our paper is finished with a conclusion section.

2. Method

Since the COVID-19 outbreak, efforts to develop deep learning techniques to perform COVID-19 screening depending on medical images, such as CT scans and chest X-rays, have increased. To describe CT sweeps of patients with COVID-19, Wu et al. set up an early screening model that is dependent on various CNN models [12]. Chest CT cuts were used by Wang et al. to propose a 3D deep CNN (DeCoVNet) to detect COVID19 [13]. Based on chest X-ray images, Chowdhury et al. used CNN to identify COVID-19 patients [14]. In other publications, 3D deep learning models have also been used to screen COVID-19 based on chest CT data [15], [16]. To assist doctors in differentiating patients with COVID-19, Yang et al. developed the Deep Pneumonia CT detection framework (based on deep learning) [17]. By modifying the origin transfer learning model to provide a clinical conclusion prior to the pathogenic test, Xu et al. established a deep learning algorithm [18]. Shi et al. used the "VB-Net" neural network to delineate the locations of COVID19 infection in CT scans [19]. A framework based on UNet++ was created by Yu et al. for the purpose of identifying COVID-19 from CT images [20]. An infection-size-aware Random Forest (iSARF) method was presented by Shen et al. and can automatically group participants into bunches depending on the size of an infected sore. For the purpose of finding the presence of COVID-19 in chest X-ray pictures, Wei Wang et al. presented an MAI-Nets model [21]. A CFW-Net deep learning model was proposed by Wei et al [22]. To identify the Covid-19, Shui-Hua developed the Wavelet Renyi Entropy and Three-Segment Biogeography-Based Optimization model [23].

2.1. Dataset preparation and preprocessing

Shen et al. introduced the infection-size-aware Random Forest (iSARF) approach, which automatically groups participants into bunches based on the size of an infected sore. Wei Wang et al. published an MAINets model to detect the presence of COVID-19 in chest X-ray images [21]. Wei et al. suggested a CFW-Net deep learning model [22]. Shui-Hua created the Wavelet Renyi Entropy and Three-Segment Biogeography-Based Optimization model [23] to find the Covid-19. In order to remove the noise caused by patients moving during analysis, we downscaled the image in this test to 128x128 and then applied the Gaussian channel. The knowledge has also been rearranged throughout the instruction at each age. The informational index is divided into two parts: training accounts for 80% and approval for 20%. From that point on, we expand the information using a variety of strategies, including flipping vertically and horizontally, rotating at various angles, shifting the width and height by around 0.2, and trimming 0.1 of the images, in order to reduce overfitting while also increasing the informational collection (Fig. 1).

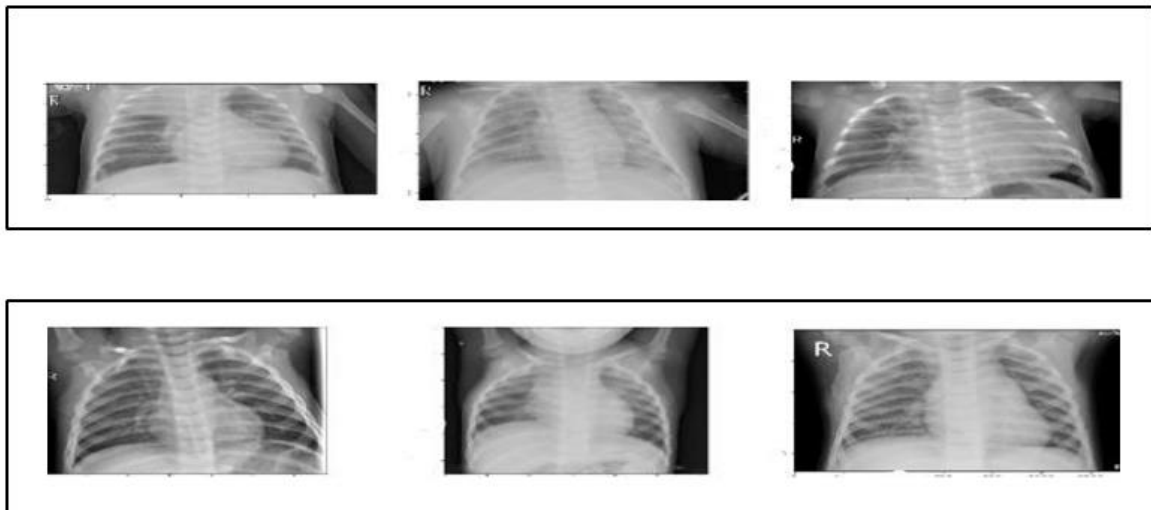


Fig. 1. Different position of sample images with Covid (up) and without Covid (down) after pre-processing.

2.2. Transfer learning

When doing transfer learning, a conventional neural architecture is used combined with pre-trained loads from large-scale datasets, such as ImageNet [24], and the loads are then adjusted for the target task. Both linguistic cognizance [25] and visual acknowledgment [26] have successfully used this idea. Transfer learning has also been widely applied to medical picture classification and acknowledgment assignments, such as tumor classification [27], the conclusion of retinal infections [28], pneumonia detection [29], and classification of skin lesion and malignant growth [10], [30]. We make use of an open source dataset [31], [32] that consists of COVID, Pneumonia, and standard X-ray pictures. There are 400 photos in the dataset. Our data is divided into three groups: 100 samples for the typical X-ray images, 100 samples for pneumonic images, and 100 samples for Covid-19 images. Fig. 2 shows various sample photos that were labeled by knowledgeable professors as normal (left) or COVID-19 cases (right).



Fig. 2. Chest X-Ray sample images: 'Normal' (left) and 'COVID-19' (right)

2.3. Dense Net-121 Architecture

A potent technology with numerous practical uses is deep neural networks (DNN) [33]. This section describes the transfer learning-based CNN model that has been certified for the classification of images as normal or COVID-19. We first re-sampled all photos to 128 128 in accordance with the architecture being used. As previously mentioned, we employed established networks like DenseNet-121 to achieve our goals of transfer learning. We may keep a wealth of knowledge for classifying different artefacts from prior training by using these well-trained networks. Layers and weights are kept in tact until the last fully linked layer.

We will update DenseNet-121 with our data. 1000 classes have been trained using DenseNet's 121 million photo database. In our instance, we have three classes and 400 photos. We replaced the last three layers with a Softmax layer to make the classification of our own dataset. (Fig. 3)

Each layer is linked to every other layer in a DenseNet architecture, giving rise to the term densely connected convolutional network. There are $L(L+1)/2$ direct connections for L layers. The feature maps of all the layers before it are used as inputs for each layer, and its own feature maps are utilized

as inputs for each layer after it. In essence, DenseNets link each layer to every other layer. The main, incredibly potent idea is this. An input layer in DenseNet is created by concatenating feature maps from earlier layers (Table.1). "DenseNets offer numerous compelling advantages: they ease the vanishing-gradient problem, strengthen feature propagation, stimulate feature reuse, and drastically reduce the number of parameters," according to the paper on densely connected convolutional networks [34].

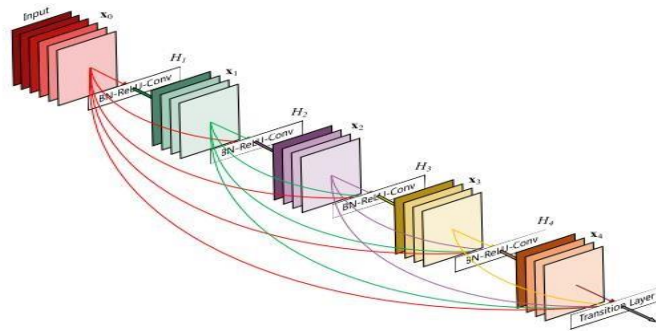


Fig. 3. DenseNet architecture

Table 1. DenseNet parameters summary

Layer (type)	Output Shape	Parameters
Efficientnet-b7	(none, 16, 16, 2560)	64097680
Global average pooling2d	(1, 1, 1, 2560)	0
Dense	(None, 104)	266344
Total parameters		64,364,024
Trainable parameters		266,344
Non-trainable parameters		64,097,680

Traditional convolutional feed-forward networks connect the output of the (L)th layer as input to the (L + 1)th layer [35] which gives rise to the following layer transition: "Eq. (1)"

$$X_L = H(X_{L-1}) \tag{1}$$

In DenseNet architecture, the dense connectivity equation is defined in "Eq. (2)":

$$X_L = H([x_0 x_1 x_2 \dots x_{L-1}]) \tag{2}$$

Where $[x_0, x_1, x_2, \dots, x_{L-1}]$ represents concatenation of the feature maps produced by $[0, 1, L]$ layers. (Fig. 4)

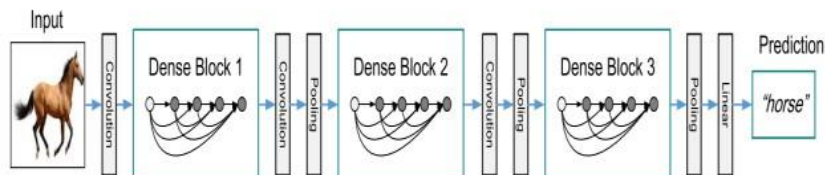


Fig. 4. A DenseNet Architecture with three (3) dense blocks [35].

2.4. Time and tools

The proposed DenseNets-121 model for COVID-19 detection is trained on Intel (R) Core(TM) i5-7200U TPU @2.75GHz, RAM (8 GB), and PYTHON 3.8 version using Google Colab . The running time was 25 minutes for the training of 400 images.

We trained our network for 60 epochs using Adam optimizer with a constant learning rate of $1e-5$. The binary cross-entropy loss function was used to calculate the loss between predictions and real labels.

3. Results and Discussion

We evaluate our model using four different metrics for each of the classes and the overall accuracy for all the classes as follows: precision: 98.33%, F1-score: 98.33% recall: 98% and an overall accuracy of 98%. (Table. 2)

Table 2. Precision, Recall, F1-score and Accuracy metrics for the proposed method

	Precision	Recall	F1-score
0	0.95	1.00	0.98
1	1.00	1.00	1.00
2	1.00	0.94	0.97
Accuracy		0.98	
Macro average		0.98	
Weighted average		0.98	

The loss vs. epochs and accuracy vs. epochs is shown in Fig. 5. The loss has converged on both the training and the validation set in 60 epochs. The accuracy on the training set is 98% and on validation set is 98%.

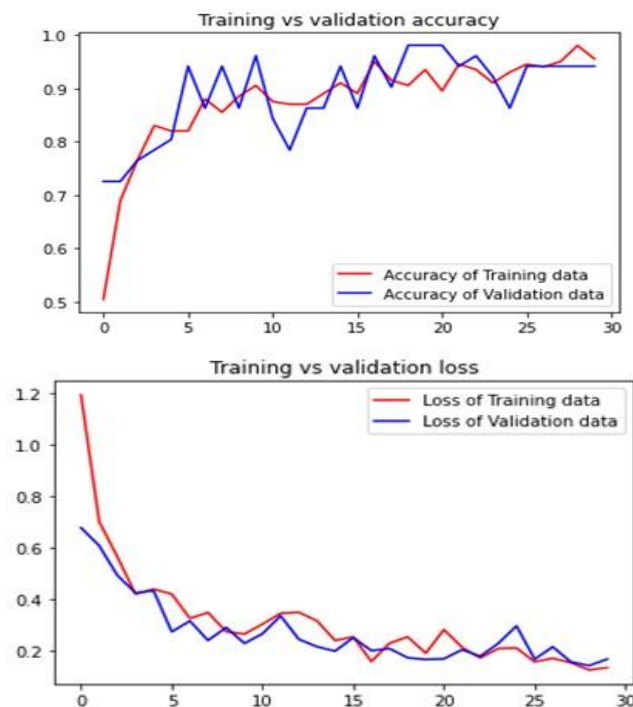


Fig. 5. Accuracy of training and validation vs. epochs (first) and loss of training and validation vs. epochs (second)

Now, if we test our model on an unseen data (Fig. 6), it will correctly classify it. Since the model was not shown the images on the validation set while training, the prediction is quite good.



Fig. 6. Testing our model on unseen data gives the correct classification.

3.1. Experiments analysis

Now that we've explained our methodology, we'll go on to the following section to talk about the model's performance in comparison to several cutting-edge models for diagnosing Covid-19 disease. (Table.3) We compute the accuracy, precision, recall, and F1score to assess the performance of the suggested model. We provide a summary definition of the metrics and discuss how they relate to our classification of novel COVID-19 disease in the paragraphs that follow. The following parameters are used to determine the metrics: TP, TN, FP, and FN stand for true positive, true negative, false positive, and false negative, respectively.

Precision: it checks what proportion of positive identifications achieved by a model were actually correct and is given by (Eq. 3).

$$Precision = \frac{TP}{(TP+FP)} \quad (3)$$

Recall: it checks the number of actual positive cases in our datasets which the proposed CNN model was able to correctly identify. This is given by (Eq. 4)

$$Recall = \frac{TP}{(TP+FN)} \quad (4)$$

F1-Score : It expresses the balance between the precision and the recall described above and helps us decide whether the performance of our model is based on precision and recall. It is given by (Eq. 5)

$$F1 - Score = \frac{2*Precision*Recall}{(Precision+Recall)} \quad (5)$$

Accuracy: Accuracy is a very popular metric that should only be used to compare distinct classes. The percentage of objects that have been accurately classified is clearly stated. It is the proportion of subjects with accurate labels to the entire group of topics. Accuracy is the most logical one (Eq. 6)

$$Accuracy = \frac{TP+TN}{(TP+TN+FP+FN)} \quad (6)$$

Specificity is the correctly items labeled by the program to all who are positive in reality. (Eq. 7)

$$Specificity = \frac{TN}{(TN+FP)} \quad (7)$$

3.2. Comparison of the approche with other Covid-19 diagnosis State-of-the-art

Compared to other approaches, our model was more accurate to classify the Covid-19 chest X-ray images. Especially where we had a leak of dataset related to this newly pandemic. Our approche could outperform the following state-of-the-art: RBFNN [36], ResNet50, InceptionV3, InceptionResNetV2 [37], 3SBBO [23], CovidResNet [38] and CovidDenseNet [39].

Accuracy = 98.00%

Precision = 98.33%

F1-score = 98.33%

Recall = 98.00%

Specificity = 96.64%

$$\text{Min} \left(\frac{TP}{(TP+FN)}, \frac{TN}{(TN+FP)} \right) = 96.64\%$$

Table 3. Performances of other convolutional neural networks to detect Covid-19 comparing our approach.

Approaches	Accuracy	Precision	F1-score	Recall	Specificity
ResNet50	93.53	96.01	94.56	96.6	90.31
Inceptio nV3	90.67	90.08	92.64	96.3	--
Inceptio nResNet V2	90.28	89.81	93.04	97.1	--
RBFNN	70.45	72.50	69.05	--	--
3SBBO	86.12	86.14	86.16	--	--
CovidRe sNet	82.46	78.67	79.35	--	--
CovidDe nseNet	82.87	79.25	80.16	82.2	--
Our approach	98.0	98.33	98.33	98.0	--

4. Conclusion

The goal of this investigation is to achieve an early detection of COVID-19 from X-ray pictures using a PCaided automated approach. In order to reduce the incidence of the virus, particularly in low-income countries, the scourge status conspiracy calls for the right X-ray examination for COVID-19 by deep learning algorithms. The view of COVID-19's X-ray images further supports the value of a CAD framework. The CNN classifier declared the results to be satisfactory with a high level of 98 percent precision. Finally, this type of architecture would be absolutely necessary for the identification of COVID-19 and for enhancing radiologists' time and effort. The proposed methodology provided an unrevealed best alternative identification technique employing a DenseNet-121 CNN, theoretically contributing to the present growing COVID-19 literature. All succeeding layers can access the feature-maps discovered by any of the DenseNet121 levels. This encourages models to be more compact and facilitates feature reuse across the network. Radiologists and professors can practically use this technique in clinical settings for precise COVID-19 detection. In order to capture a real-picture of infection rate, which has a high association to the number of daily-infected cases, boosting dependability represented through the proposed computational approach for testing could be valuable. The used methodology provided a potent machine learning-based strategy to reduce manual judgment errors made by professionals and provide a quicker way of offering time and resource saving. Applying various types of architecture, such as DenseNet-161, DenseNet-169, and DenseNet-201, can support DenseNet-121 for future research development. To identify COVID-19 patients more precisely, alternative deep learning techniques or modified deep learning techniques could be used and tested for future development and assessment.

Acknowledgment

We would like to thank Google for providing free and powerful GPU on Colab servers and free space on Google Drive. As well as the Python community and open access, Github for database free downloading.

References

- [1] “Weekly epidemiological update on COVID-19 - 8 June 2021.” Available at : <https://www.who.int/publications/m/item/weekly-epidemiological-update-on-covid-19--8-june-2021>.
- [2] C. Huang *et al.*, “Clinical features of patients infected with 2019 novel coronavirus in Wuhan, China,” *Lancet*, vol. 395, no. 10223, pp. 497–506, Feb. 2020, doi: [10.1016/S0140-6736\(20\)30183-5](https://doi.org/10.1016/S0140-6736(20)30183-5).
- [3] W. Guan *et al.*, “Clinical characteristics of 2019 novel coronavirus infection in China,” *medRxiv*, p. 2020.02.06.20020974, Feb. 2020, doi: [10.1101/2020.02.06.20020974](https://doi.org/10.1101/2020.02.06.20020974).
- [4] J. Lei, J. Li, X. Li, and X. Qi, “CT imaging of the 2019 novel coronavirus (2019-NCoV) pneumonia,” *Radiology*, vol. 295, no. 1, p. 18, Jan. 2020, doi: [10.1148/RADIOL.2020200236](https://doi.org/10.1148/RADIOL.2020200236).
- [5] F. Song *et al.*, “Emerging 2019 novel coronavirus (2019-NCoV) pneumonia,” *Radiology*, vol. 295, no. 1, pp. 210–217, Feb. 2020, doi: [10.1148/RADIOL.2020200274](https://doi.org/10.1148/RADIOL.2020200274).
- [6] M. Chung *et al.*, “CT imaging features of 2019 novel coronavirus (2019-NCoV),” *Radiology*, vol. 295, no. 1, pp. 202–207, Feb. 2020, doi: [10.1148/RADIOL.2020200230](https://doi.org/10.1148/RADIOL.2020200230).
- [7] D. Ardila *et al.*, “End-to-end lung cancer screening with three-dimensional deep learning on low-dose chest computed tomography,” *Nat. Med.* 2019 256, vol. 25, no. 6, pp. 954–961, May 2019, doi: [10.1038/s41591-019-0447-x](https://doi.org/10.1038/s41591-019-0447-x).
- [8] K. Suzuki, “Overview of deep learning in medical imaging,” *Radiol. Phys. Technol.*, vol. 10, no. 3, pp. 257–273, Sep. 2017, doi: [10.1007/S12194-017-0406-5](https://doi.org/10.1007/S12194-017-0406-5).
- [9] N. Coudray *et al.*, “Classification and mutation prediction from non-small cell lung cancer histopathology images using deep learning,” *Nat. Med.* 2018 2410, vol. 24, no. 10, pp. 1559–1567, Sep. 2018, doi: [10.1038/s41591-018-0177-5](https://doi.org/10.1038/s41591-018-0177-5).
- [10] A. Esteva *et al.*, “Dermatologist-level classification of skin cancer with deep neural networks,” *Nat.* 2017 5427639, vol. 542, no. 7639, pp. 115–118, Jan. 2017, doi: [10.1038/nature21056](https://doi.org/10.1038/nature21056).
- [11] H. Kaiming, Z. Xiangyu, R. Shaoqing, and S. Jian, “Delving Deep into Rectifiers: Surpassing Human-Level Performance on ImageNet Classification Kaiming,” *Biochem. Biophys. Res. Commun.*, vol. 498, no. 1, pp. 254–261, 2018. doi : [10.48550/arXiv.1502.01852](https://doi.org/10.48550/arXiv.1502.01852).
- [12] X. Xu *et al.*, “A Deep Learning System to Screen Novel Coronavirus Disease 2019 Pneumonia,” *Engineering*, vol. 6, no. 10, pp. 1122–1129, Oct. 2020, doi: [10.1016/J.ENG.2020.04.010](https://doi.org/10.1016/J.ENG.2020.04.010).
- [13] C. Zheng *et al.*, “Deep Learning-based Detection for COVID-19 from Chest CT using Weak Label,” *medRxiv*, p. 2020.03.12.20027185, Mar. 2020, doi: [10.1101/2020.03.12.20027185](https://doi.org/10.1101/2020.03.12.20027185).
- [14] M. E. H. Chowdhury *et al.*, “Can AI Help in Screening Viral and COVID-19 Pneumonia?,” *IEEE Access*, vol. 8, pp. 132665–132676, 2020, doi: [10.1109/ACCESS.2020.3010287](https://doi.org/10.1109/ACCESS.2020.3010287).
- [15] O. Gozes *et al.*, “Rapid AI Development Cycle for the Coronavirus (COVID-19) Pandemic: Initial Results for Automated Detection & Patient Monitoring using Deep Learning CT Image Analysis,” Mar. 2020, Accessed: Apr. 20, 2023. doi: [10.48550/arXiv.2003.05037](https://doi.org/10.48550/arXiv.2003.05037).
- [16] L. Li *et al.*, “Artificial Intelligence Distinguishes COVID-19 from Community Acquired Pneumonia on Chest CT,” *Radiology*, vol. 296, no. 2, pp. E65–E71, Aug. 2020, doi: [10.1148/RADIOL.2020200905](https://doi.org/10.1148/RADIOL.2020200905).
- [17] Y. Song *et al.*, “Deep Learning Enables Accurate Diagnosis of Novel Coronavirus (COVID-19) With CT Images,” *IEEE/ACM Trans. Comput. Biol. Bioinforma.*, vol. 18, no. 6, pp. 2775–2780, 2021, doi: [10.1109/TCBB.2021.3065361](https://doi.org/10.1109/TCBB.2021.3065361).
- [18] S. Wang *et al.*, “A deep learning algorithm using CT images to screen for Corona Virus Disease (COVID-19),” *medRxiv*, p. 2020.02.14.20023028, Apr. 2020, doi: [10.1101/2020.02.14.20023028](https://doi.org/10.1101/2020.02.14.20023028).
- [19] F. Shan *et al.*, “Lung Infection Quantification of COVID-19 in CT Images with Deep Learning,” *Med. Phys.*, vol. 48, no. 4, pp. 1633–1645, Mar. 2020, doi: [10.1002/mp.14609](https://doi.org/10.1002/mp.14609).
- [20] J. Chen *et al.*, “Deep learning-based model for detecting 2019 novel coronavirus pneumonia on high-resolution computed tomography,” *Sci. Reports* 2020 101, vol. 10, no. 1, pp. 1–11, Nov. 2020, doi:

[10.1038/s41598-020-76282-0](https://doi.org/10.1038/s41598-020-76282-0).

- [21] W. Wang, X. Huang, J. Li, P. Zhang, and X. Wang, "Detecting COVID-19 Patients in X-Ray Images Based on MAI-Nets," *Int. J. Comput. Intell. Syst.*, vol. 14, no. 1, pp. 1607–1616, May 2021, doi: [10.2991/IJCIS.D.210518.001](https://doi.org/10.2991/IJCIS.D.210518.001).
- [22] W. Wang, H. Liu, J. Li, H. Nie, and X. Wang, "Using CFW-Net Deep Learning Models for X-Ray Images to Detect COVID-19 Patients," *Int. J. Comput. Intell. Syst.*, vol. 14, no. 1, pp. 199–207, Nov. 2020, doi: [10.2991/IJCIS.D.201123.001](https://doi.org/10.2991/IJCIS.D.201123.001).
- [23] S. H. Wang, X. Wu, Y. D. Zhang, C. Tang, and X. Zhang, "Diagnosis of COVID-19 by Wavelet Renyi Entropy and Three-Segment Biogeography-Based Optimization," *Int. J. Comput. Intell. Syst.*, vol. 13, no. 1, pp. 1332–1344, Sep. 2020, doi: [10.2991/IJCIS.D.200828.001](https://doi.org/10.2991/IJCIS.D.200828.001).
- [24] J. Deng, W. Dong, R. Socher, L.-J. Li, Kai Li, and Li Fei-Fei, "ImageNet: A large-scale hierarchical image database," pp. 248–255, Mar. 2010, doi: [10.1109/CVPR.2009.5206848](https://doi.org/10.1109/CVPR.2009.5206848).
- [25] J. Devlin, M. W. Chang, K. Lee, and K. Toutanova, "BERT: Pre-training of Deep Bidirectional Transformers for Language Understanding," *NAACL HLT 2019 - 2019 Conf. North Am. Chapter Assoc. Comput. Linguist. Hum. Lang. Technol. - Proc. Conf.*, vol. 1, pp. 4171–4186, Oct. 2018, Accessed: Apr. 20, 2023. doi : [10.48550/arXiv.1810.04805](https://doi.org/10.48550/arXiv.1810.04805).
- [26] S. Ren, K. He, R. Girshick, and J. Sun, "Faster R-CNN: Towards Real-Time Object Detection with Region Proposal Networks," *IEEE Trans. Pattern Anal. Mach. Intell.*, vol. 39, no. 6, pp. 1137–1149, Jun. 2015, doi: [10.1109/TPAMI.2016.2577031](https://doi.org/10.1109/TPAMI.2016.2577031).
- [27] B. Q. Huynh, H. Li, and M. L. Giger, "Digital mammographic tumor classification using transfer learning from deep convolutional neural networks," vol. 3, no. 3, p. 034501, Aug. 2016, doi: [10.1117/1.JMI.3.3.034501](https://doi.org/10.1117/1.JMI.3.3.034501).
- [28] M. Raghu, C. Zhang, J. Kleinberg, and S. Bengio, "Transfusion: Understanding Transfer Learning for Medical Imaging," *Adv. Neural Inf. Process. Syst.*, vol. 32, Feb. 2019, Accessed: Apr. 20, 2023. doi: [10.48550/arXiv.1902.07208](https://doi.org/10.48550/arXiv.1902.07208).
- [29] V. Chouhan *et al.*, "A Novel Transfer Learning Based Approach for Pneumonia Detection in Chest X-ray Images," *Appl. Sci. 2020, Vol. 10, Page 559*, vol. 10, no. 2, p. 559, Jan. 2020, doi: [10.3390/APP10020559](https://doi.org/10.3390/APP10020559).
- [30] M. S. Elmahdy, S. S. Abdeldayem, and I. A. Yassine, "Low quality dermal image classification using transfer learning," *2017 IEEE EMBS Int. Conf. Biomed. Heal. Informatics, BHI 2017*, pp. 373–376, Apr. 2017, doi: [10.1109/BHI.2017.7897283](https://doi.org/10.1109/BHI.2017.7897283).
- [31] X. Yang, X. He, J. Zhao, Y. Zhang, S. Zhang, and P. Xie, "COVID-CT-Dataset: A CT Scan Dataset about COVID-19," Mar. 2020, Accessed: Apr. 20, 2023. doi: [10.48550/arXiv.2003.13865](https://doi.org/10.48550/arXiv.2003.13865).
- [32] P. Sudowe and B. Leibe, "Patchit: Self-supervised network weight initialization for fine-grained recognition," *Br. Mach. Vis. Conf. 2016, BMVC 2016*, vol. 2016-September, pp. 2266–2270, 2016, doi: [10.5244/C.30.75](https://doi.org/10.5244/C.30.75).
- [33] S. B. Belhaouari and H. Raissouli, "MADL: A Multilevel Architecture of Deep Learning," *Int. J. Comput. Intell. Syst.*, vol. 14, no. 1, pp. 693–700, Feb. 2021, doi: [10.2991/IJCIS.D.201216.003](https://doi.org/10.2991/IJCIS.D.201216.003).
- [34] G. Huang, Z. Liu, L. Van Der Maaten, and K. Q. Weinberger, "Densely connected convolutional networks," *Proc. - 30th IEEE Conf. Comput. Vis. Pattern Recognition, CVPR 2017*, vol. 2017-January, pp. 2261–2269, Nov. 2017, doi: [10.1109/CVPR.2017.243](https://doi.org/10.1109/CVPR.2017.243).
- [35] A. Krizhevsky, I. Sutskever, and G. E. Hinton, "ImageNet classification with deep convolutional neural networks," *Commun. ACM*, vol. 60, no. 6, pp. 84–90, May 2017, doi: [10.1145/3065386](https://doi.org/10.1145/3065386).
- [36] K. He, X. Zhang, S. Ren, and J. Sun, "Deep residual learning for image recognition," *Proc. IEEE Comput. Soc. Conf. Comput. Vis. Pattern Recognit.*, vol. 2016-December, pp. 770–778, Dec. 2016, doi: [10.1109/CVPR.2016.90](https://doi.org/10.1109/CVPR.2016.90).
- [37] N. S. Punn and S. Agarwal, "Automated diagnosis of COVID-19 with limited posteroanterior chest X-ray images using fine-tuned deep neural networks," *Appl. Intell.*, vol. 51, no. 5, pp. 2689–2702, May 2021, doi: [10.1007/S10489-020-01900-3](https://doi.org/10.1007/S10489-020-01900-3).

-
- [38] N. Narayan Das, N. Kumar, M. Kaur, V. Kumar, and D. Singh, "Automated Deep Transfer Learning-Based Approach for Detection of COVID-19 Infection in Chest X-rays," *IRBM*, vol. 43, no. 2, pp. 114–119, Apr. 2022, doi: [10.1016/J.IRBM.2020.07.001](https://doi.org/10.1016/J.IRBM.2020.07.001).
- [39] H. Alshazly, C. Linse, M. Abdalla, E. Barth, and T. Martinetz, "COVID-Nets: Deep CNN Architectures for Detecting COVID-19 Using Chest CT Scans," *medRxiv*, p. 2021.04.19.21255763, Apr. 2021, doi: [10.1101/2021.04.19.21255763](https://doi.org/10.1101/2021.04.19.21255763).